Magnetic field driven redistribution between extended and localized electronic states in high-mobility Si MOSFETs at low temperatures

V. M. Pudalov [1,3] and M. E. Gershenson [2]
[1] *V. L. Ginzburg Research Center for High Temperature Superconductivity and Quantum Materials, P. N. Lebedev Physical Institute, 119991 Moscow, Russia*
[2] *Serin Physics Lab, Rutgers University, Piscataway New Jersey 08854, USA*
[3] *HSE University, 101000 Moscow, Russia*

(Received 11 February 2021; revised 21 June 2021; accepted 23 June 2021; published 6 July 2021)

In the study of oscillatory electron transport in high-mobility Si MOSFETs at low temperatures we observe two correlated effects in weak in-plane magnetic fields: a steep decrease of the magnetic susceptibility $\chi^*(H)$ and an increase of the concentration of mobile carriers $n(H)$. We suggest a phenomenological model of the magnetic field driven redistribution between the extended and localized electronic states that qualitatively explains both effects. We argue that the redistribution is mainly caused by magnetization of the large-spin $S \approx 2$ localized states with energies close to the Fermi energy E_F, coexisting with the majority Fermi liquid state. Our findings also resolve a long-standing disagreement between the experimental data on χ^* obtained in weak ($H \sim k_B T/\mu_B$) and strong ($H \sim E_F/g\mu_B$) magnetic fields.

DOI: 10.1103/PhysRevB.104.035407

I. INTRODUCTION

Dilute two-dimensional systems of electrons represent a very fruitful playground for exploration of the physics of strongly interacting charged fermions. The conventional approach, i.e., the Landau theory of Fermi liquids (FL), treats the system of interacting electrons as a gas of quasi-electrons whose parameters are renormalized by interactions [1,2]. It is, however, questionable whether this description remains valid for a two-dimensional (2D) system when the electron-electron interaction energy E_{ee} greatly exceeds the Fermi energy E_F [3], i.e., at $r_s \gg 1$ [4]. Different approaches to this problem gave birth to a plethora of theoretical suggestions [5–9] for the ground states of strongly interacting electron systems.

Various correlated systems close to the Mott transition exhibit a tendency to phase separate in insulator and metallic phases with different densities [10]. This tendency is suppressed by the long-range Coulomb interaction and by the gate screening (for the 2D gated systems), which favors uniform phases. Spatial phase separation and the emergence of an inhomogeneous state also often occurs in the vicinity of a phase transition, e.g., between superconducting, normal, and magnetically ordered phases [11,12]. More specifically, for a two-dimensional hole system, using the local compressibility measurements Ilani *et al.* [13] observed the emergence of an inhomogeneous state in the vicinity of the metal-to-insulator transition.

The anomalous spin magnetization observed in the in-plane magnetic fields for the strongly correlated system in thermodynamic magnetization [14] and anomalous magneto-transport [15,16] were interpreted as a transition of a dilute 2D system into the two-phase state. In the two-phase state, the large-spin collective localized states, the so-called spin droplets (SD), emerge and coexist with FL of mobile electrons. The total spin of an individual droplet, $S = 2$ [14], is almost independent of the carrier density and temperature, whereas the number of droplets per unit area strongly depends on the temperature and the electron density [15]. The idea of the large-spin droplets has received theoretical support [17].

The disorder-enhanced magnetism in the ground state for restricted geometries has been considered in Refs. [18–20]. Formation of local regions with nonzero spin density in a disordered 2D system close to the Stoner instability was predicted in Ref. [21]. On the other hand, the two-phase state was suggested to emerge from a pure 2D Fermi liquid on the verge of the Wigner crystallization [5]. Electron and hole puddles, coupled by tunneling to the edge states, are believed to be a common feature of 2D topological insulators [22,23]. Recently, the mesoscopic Stoner instability in open quantum dots, tunnel-coupled to external fermionic reservoir, was studied theoretically in Ref. [24]. On the experimental side, for mesoscopic size samples, a phase-inhomogeneous state was observed by the authors of Ref. [25]; signatures of spin polarization for a confined few-electrons system reported in Refs. [26,27] were considered as evidence of interaction-induced collective spin polarization transition.

In the current paper we report evidence for the presence of inhomogeneous two-phase state over a wide range of carrier concentrations on the "metallic" side of the so-called "2D metal-insulator" transition in macroscopic 2D electron system in (100) Si-MOS structures. Our detailed measurements of the Shubnikov–de Haas (ShdH) oscillations in vector magnetic fields revealed steep variations of (i) the renormalized spin susceptibility $\chi^*(H)$ and (ii) the mobile carrier density $n_{\mathrm{SdH}}(H)$, driven by a weak in-plane field $H_\parallel$. The unexpected nonmonotonic variations of the susceptibility (∼10–20%)

and 2D carrier density (∼3%) correlate with each other and with thermodynamic spin magnetization of electrons. These correlations allowed us to identify the origin of these effects.

We associate the density variation with the magnetic field driven redistribution of electrons between two phases of different electron states. The majority phase is the 2D Fermi liquid of mobile electrons, for which the local carrier density can be determined from the SdH oscillations. The minority phase, we believe, consists of the collective localized spin droplets [14] which are imbedded in the 2D Fermi liquid.

We show that in the studied two-phase system the carrier redistribution between the two states is driven by the magnetization of the large-spin SD states in the in-plane magnetic field $H_\parallel$. We tested this idea by considering a phenomenological thermodynamic model of the two-phase state and linked the observed changes in the nonlinear SD magnetization with changes in the FL density $n_{\rm SdH}(H_\parallel)$ and susceptibility $\chi^*(H_\parallel)$. The observed $\chi^*(H_\parallel)$ dependence indicates that a widely employed technique of extracting the 2D spin susceptibility from measurements of the magnetoresistance saturation [28,29] may provide inaccurate results not only when measurements are performed in the strong fields of the order of $E_F/g\mu_B$ (as noted in Ref. [30]), but already in a much weaker field of the order of temperature.

II. EXPERIMENT

The ac (13 Hz) transport measurements were performed with two (100) Si-MOS samples from different wafers Si6-14 and Si3-10 with the peak mobility 2.4 m^2/Vs and 3.2 m^2/Vs, respectively (at $T = 0.3$ K). For the resistivity ρ_{xx} measurements we used the vector magnetic field technique with two independent superconducting coils. Typical examples of the SdH oscillations at different in-plane fields and their fitting may be found in Refs. [31–33]. The oscillatory component $\delta\rho_{xx}$ was shown earlier to be well fitted with conventional Lifshits-Kosevich formula [31,33,34]; this enables accurate extraction of χ^* and $n_{\rm SdH}$. In particular, χ^* values were determined from the oscillation beating with an accuracy of ∼(1–2)%.

The results were available within the temperature range $T < 0.5K$, in which the ShdH oscillations in weak $H_\perp$ fields [32] are not damped by temperature. The new data reported here coincide in the $H_\parallel \to 0$ limit with the $\chi^*(0)$ values reported earlier in Refs. [32,35].

III. RESULTS

Figure 1 shows an unexpected nonmonotonic dependence of χ^* on the in-plane field. This dependence is reproducible for both samples studied. As the density increases from $n = 0.99$ to 10×10^{11}cm^{-2}, the $\delta\chi^*(H)/\chi^*(0)$ variations decrease from ∼25% to ∼(10–6)%. The characteristic field of the $\chi^*(H)$-minimum, $H_\parallel \sim 1$ T for $n = (1.1–2) \times 10^{11}$cm^{-2}, is much weaker than the field of complete spin polarization of the 2D system, $H_p = 2E_F/g^*\mu_B$ (∼20T for $n = 2 \times 10^{11}$cm^{-2}). We note that in a homogeneous single-phase FL system H_p is the only characteristic field.

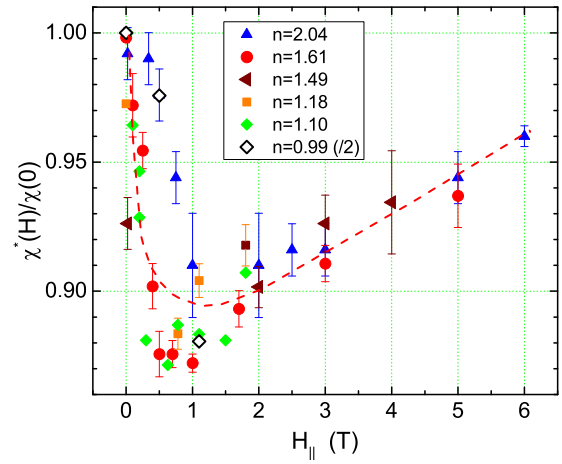

FIG. 1. Summary of $\chi^*(H_\parallel)/\chi^*(0)$ data versus $H_\parallel$ for both samples and for several densities. For the lowest density $n = 0.99$, the $\chi^*(H)/\chi^*(0)$ variations are scaled down by two times. The density is indicated in units of 10^{11} cm^{-2}, $T = 0.1$ K. The dashed line is a guide to the eye.

The hint for explanation of the puzzling $\chi^*(H_\parallel)$ field dependence is provided by the observed remarkable correlation between the spin susceptibility minimum and the maximum of the mobile carrier density, determined from the SdH oscillation frequency in weak tilted fields (see Fig. 2). Though the density changes $\delta n_{\rm SdH}/n_{\rm SdH}$ are small, ∼2%, they are reliably determined for various densities. The correlation has been observed over the whole studied range of densities. Since the total charge of the gated structure is conserved, the observed dependence $\delta n_{\rm SdH}(H)$ provides evidence for the field-induced redistribution between the localized and extended electronic states.

Both sharp field dependencies of the spin susceptibility $\chi^*(H)/\chi^*(0)$ and the density of mobile carriers $n_{\rm SdH}(H)$ were measured simultaneously in the same experiment, from the beating pattern of SdH oscillations in vector fields, and are in remarkable correlation with each other. Such "generic" V- and Λ-shaped dependencies have been observed over the range of densities $(1.1–2.1) \times 10^{11}$ cm^{-2} (referred to as "intermediate" densities); they are qualitatively similar for the two studied samples.

Below we describe more complex behavior of $\chi^*(H)$ and $n_{\rm SdH}(H)$ over the extended range of densities.

A. Low densities

For the lowest density $n = 0.99 \times 10^{11}$ cm^{-2} the drop $\delta\chi^*$ with $H_\parallel$ is surprisingly prominent (25%), as Fig. 3(a) shows. At such low densities on the verge of the transition to fully localized state, the $n_{\rm SdH}(H)$ variation could not be measured and variations of $\chi^*(H)$ could not be traced to higher field because application of an in-plane field caused complete localization of the 2D system [36–39].

B. High densities

The $\delta\chi^*/\chi(0)$ variations become smaller with increasing density: e.g., at $n = 6.16 \times 10^{11}$ cm^{-2} the drop becomes a

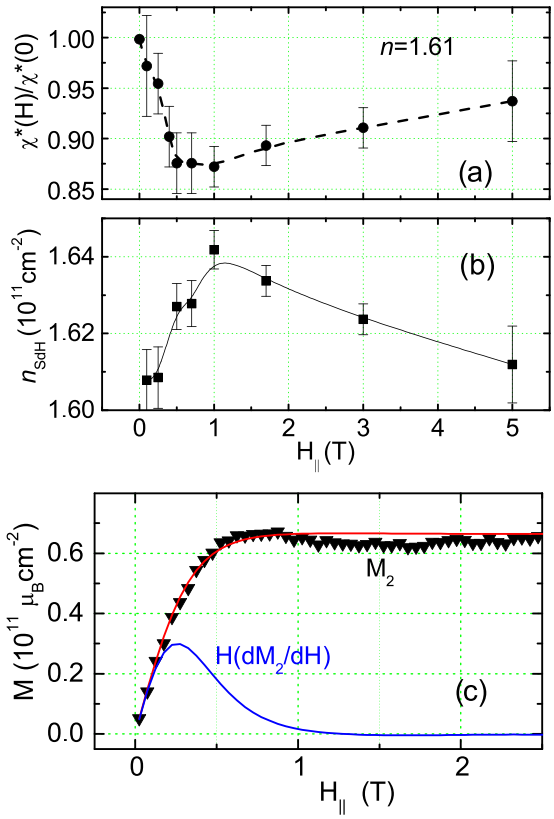

FIG. 2. Correlation between the in-plane field dependence of (a) $\chi^*(H)/\chi^*(0)$, (b) density n_{SdH}, and (c) spin magnetization $M(H_\parallel)$ (reproduced from Ref. [31]). Red curve shows $\tanh(\mu_B H/k_B T)$-fitting of the experimental $M(H)$ data, blue curve shows $H\partial M/\partial H$ calculated from the fitting curve. The zero-field density $n_0 = 1.61 \times 10^{11}\,\mathrm{cm}^{-2}$ for (a) and (b), and $1.4 \times 10^{11}\,\mathrm{cm}^{-2}$ for (c). Temperature $T = 0.1$ K for (a) and (b) and 1.7 K for (c).

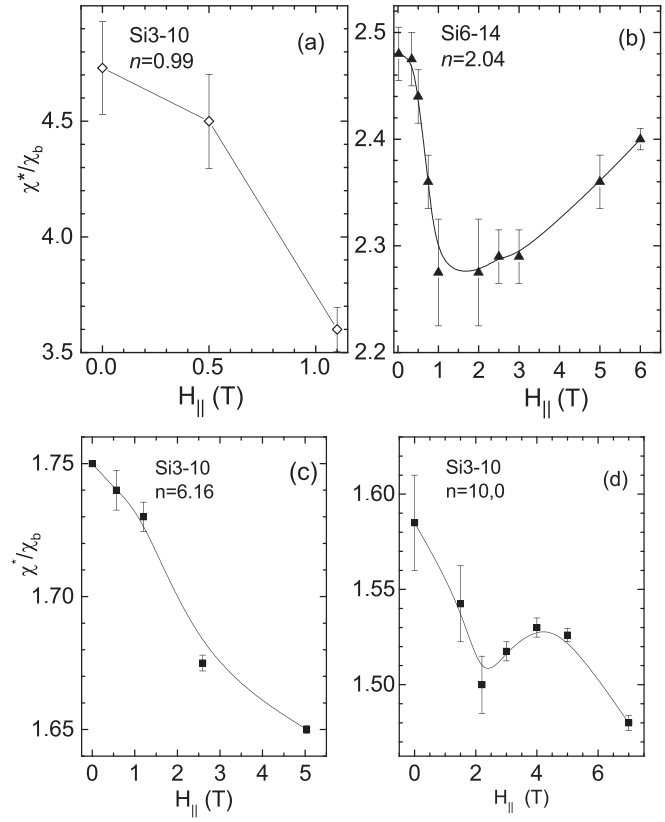

FIG. 3. Evolution of the $\chi^*(H)/\chi_b$ dependencies with density, from the (a) lowest density $0.99 \times 10^{11}\,\mathrm{cm}^{-2}$ to higher densities (b) $2 \times 10^{11}\,\mathrm{cm}^{-2}$, (c) $6.16 \times 10^{11}\,\mathrm{cm}^{-2}$, and at the highest studied density (d) $10.0 \times 10^{11}\,\mathrm{cm}^{-2}$.

factor of 4 weaker than that for $0.99 \times 10^{11}\,\mathrm{cm}^{-2}$ [compare Figs. 3(a) and 3(c)]. For even a higher density $10 \times 10^{11}\,\mathrm{cm}^{-2}$, $\chi^*(H)$ continues decreasing with field, and its overall change does not exceed ≈6%, [see Figs. 3(c) and 3(d)]. The minimum $\chi^*(H)$ shifts toward stronger fields, and the V-shape is replaced with a more complex nonmonotonic dependence. Figure 4 shows that the concomitant $n(H)$ dependence also changes from Λ-shaped to a more complex one, and the initial rise of $n(H)$ is replaced with the $n(H)$ decrease in weak fields. Though the shapes of the dependencies $n(H)$ and $\chi^*(H)$ become more complex, the correlations between them persist (Fig. 5). This case is discussed below.

IV. CONCLUSIONS DRAWN FROM DATA

(1) The observed small (2%) density variation [Fig. 2(b)] cannot be the driving force behind the ∼13% variations of $\chi^*(H_\parallel)$ [Fig. 2(a)]. Indeed, one might expect $(\partial \ln \chi^*/\partial H)$ to be only ≈0.6% per Tesla for $n = 1.5 \times 10^{11}\,\mathrm{cm}^{-2}$, estimated using the measured $\partial\chi^*/\partial n$ value from Ref. [32]. Thus, the observed $\delta n_{\mathrm{SdH}}(H)$ should be considered as a concomitant effect rather than the main reason for $\chi^*(H)$ variation.

(2) The spin susceptibility variations $\delta\chi^*(H)$ measured from SdH oscillations are relevant to the mobile carriers. This data also correlate with with thermodynamic magnetization data [see Fig. 2(c)], which is determined mainly by the large-spin collective localized states [14]. Thus, we believe that the observed changes in the properties of extended states are caused by the magnetization changes of the localized states and by the subsequent carriers redistribution between the two subsystems.

(3) The energy of the localized states must be located in the close vicinity of the Fermi energy to allow for the carrier exchange at ultralow temperatures between two electronic phases. We refer to these states as "fast" localized states. No temperature dependence of δn_{SdH} was observed within the range 0.1–0.5 K, therefore we believe that the carrier redistribution occurs elastically, via tunneling. The corresponding energy diagram for the two states is schematically shown in Fig. 6(c). Note, that this picture is different from the conventional model of the disorder-localized single-particle states in the tail of the conduction band [40–42].

(4) The considered "fast" localized states are of a 2D nature and, hence, are a part of the 2D electron system rather than three-dimensional (3D) interface states because both n_{SdH} and χ^* changes are observed only in the in-plane field.

V. DATA OVERVIEW

Our measurements were performed at a fixed gate voltage V_g, whereas $H_\parallel$ and T have been varied. Under this condition

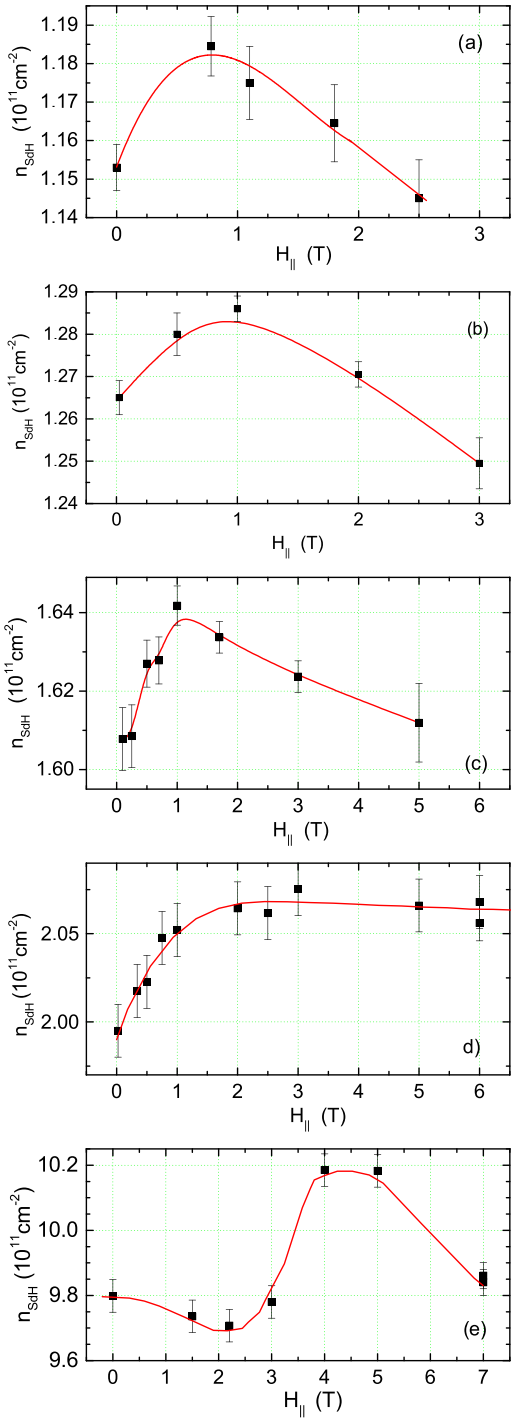

FIG. 4. Density variations as a function of the in-plane magnetic field $H_{||}$ for the zero-field densities $n_{SdH}(0)$: (a) 1.153, (b) 1.265, (c) 1.64, (d) 2.0, and (e) 9.8×10^{11} cm^{-2}.

the total charge is conserved. The total charge in the multicomponent system includes both the extended ("mobile") and localized electron states. Only the "mobile" carriers contribute to the SdH oscillations; their local density is experimentally found from the oscillations frequency.

The localized states include "fast" and "slow" localized states. The former states are capable of recharging and reaching equilibrium with the extended states at the ms-timescale

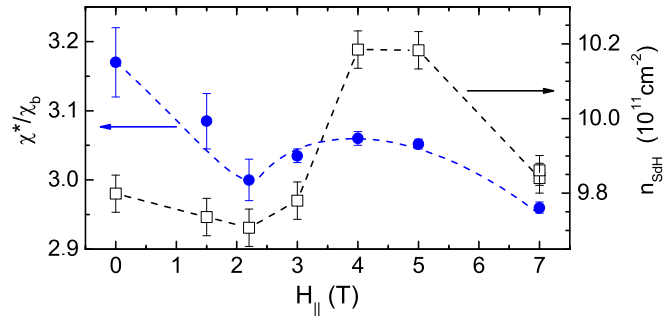

FIG. 5. Comparison of the magnetic field dependences of $\chi^*(H)/\chi_b$ and $n(H)$ at high carrier density $n \approx 10 \times 10^{11}$ cm^{-2}. Sample Si3-10.

after changing the gate voltage, magnetic field and temperature [14,43]. We associate the "fast" localized states with collective "spin droplets" possessing large spins. Such a conclusion, consistent with that found in Ref. [14], is based on (i) the observation of the large thermodynamic spin magnetization exceeding the Bohr magneton [14], fast increase of the magnetization energy with field, and (ii) the low value of the characteristic field of the magnetization saturation $H \sim 0.25 k_B T/\mu_B \approx 1$ T [see Fig. 2(c)]. The magnetization resembles that of free spins $M \propto \tanh(\mu_B H/k_B T)$, but saturates in the field $H_{||} \approx (0.8–1)$T, which is four times weaker than that anticipated for free spin-1/2 electrons; this observation points at a large total spin $S \approx 2$ of the collective state [14].

In contrast, the "slow" single-particle localized states (SPL), which are positioned deeply below the Fermi energy, in the tail of the conduction band, do not recharge within the time of measurements; they do not participate in low-temperature transport and equilibrium thermodynamics. Their presence may be revealed, e.g., by polarizing the system with the

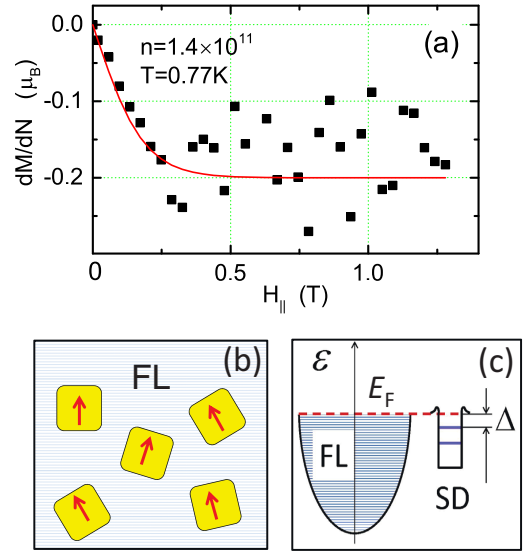

FIG. 6. (a) dM/dN versus $H_{||}$. Symbols are the data from Ref. [31] for $n = 1.4 \times 10^{11}$ cm^{-2}. (b), (c) Schematic spatial arrangement of the two-phase state and the energy band diagram of the two-phase system.

in-plane field [41,42]. Since the SPL states are not recharging in the described measurements, we will not discuss them below. Correspondingly, we assume, $\delta N_{\rm mob} + \delta N_{\rm loc} = 0$ for the two-component system, where the electron densities δN_i in the two phases are functions of the temperature and magnetic field. We show below that the minimal phenomenological model involving these two components is capable of explaining our results qualitatively.

VI. MODEL

In Appendixes A and B to this paper we consider the spin susceptibility variations within the theory of interaction quantum corrections and the conventional thermodynamics of the single-phase state. We show that these effects cannot explain the reported experimental data. Moreover, the observed magnetic field variation of the mobile carrier density under fixed total charge in the gated structure is a clear indication of the presence of two phases in the studied electron system. For this reason we consider below the phenomenology of the phase separated two-phase state.

We conclude that the predicted magnetic field dependencies due to interaction corrections and spin-polarization are irrelevant (to the first approximation) to the observed sharp changes of $\chi^*(H)$.

A. Thermodynamics of the two-phase state

In the phenomenological model proposed below, for simplicity, we neglected both monotonic quantum corrections and the dependence of χ^* on the degree of spin polarization.

Let us denote $A_{\rm FL} \equiv A_1$ – the fraction of the total area occupied by the FL states and $A_{\rm SD} = A_2$ — the fraction of the total area occupied by the collective localized states (spin droplets, SD). $A_{\rm SD} + A_{\rm FL} = 1$, if one ignores the presence of the single-particle localized (SPL) states (this can be justified since they do not recharge and do not thermalize during measurements). As long as the 2D system is conductive, the percolating-type arguments suggest that the FL phase is the majority phase and occupies more than 50% of the sample's area., i.e., $A_{\rm SD} < A_{\rm FL}$.

The number of electrons per unit area in each phase is $N_1 \equiv N_{\rm FL}$ and $N_2 \equiv N_{\rm loc}$, and $n_{\rm FL}$ and $n_{\rm SD}$ correspond to the local densities of the states in the regions occupied by FL and SD phases. On the spatial scale shorter than the distance between the gate and the 2D layer ($\approx$200 nm) the local densities in these two phases may only insignificantly differ from each other and from the average density, both being dependent on external parameters. The areal density of electrons (i.e., per unit area of the overall 2D system) in each phase is $N_i = n_i A_i$. Then the total charge of the 2D system

$$Q/e \equiv N = N_1 + N_2 = n_{\rm FL} A_{\rm FL} + n_{\rm SD} A_{\rm SD}. \qquad (1)$$

The gate voltage controls N rather than n_i when the total 2D system is recharged. Correspondingly, for the two-component system at a fixed gate voltage V_g, $\delta N_{\rm FL} + \delta N_{\rm loc} = 0$, where δN_i are functions of temperature and field. The thermodynamic magnetization measurements [14] show that the individual spin droplet size is independent of N, T, and H. Hence the local density $n_{\rm SD}$ also remains constant, whereas $n_{\rm FL}$ and A_i may vary with N, T, and H. Based on the electrostatic arguments, we assume that N depends only on V_g, being independent of H and T.

There is a fundamental difference between the parameters probed by the transport and thermodynamic measurements. From frequency of the SdH oscillations one determines (i) the local density of electrons participating in the cyclotron motion $n_{\rm SdH} \equiv n_{\rm FL} = N_1/A_1$ and (ii) χ^* the spin susceptibility of mobile electrons. On the other hand, both phases contribute to the thermodynamic magnetization, whose measurements provide $d\mu/dH = -dM/dN$ and $M = \int (dM/dN) dN$ (M is roughly proportional to $N_2 = n_{\rm SD} \times A_2$ because the magnetization of the FL state is significantly smaller at low and intermediate carrier densities). Similarly, the capacitive-type measurements performed at low frequencies, $\ll 10^{11}$ Hz, probe all carriers, including SD and mobile FL states.

1. *On the origin and structure of the localized states*

In the absence of direct microscopic data on the spatial extension of the spin droplets (SD) and their energy spectrum, we can only conjecture on the SD origin. The size of the spin droplet was estimated in Ref. [14] as $\sqrt{2S/n}$, that is $\sim$(40–100) nm for the total spin $S = 2$ and density $n = (0.5\text{–}2) \times 10^{11}\,{\rm cm}^{-2}$. This size is comparable with the gate oxide thickness of 200 nm; at greater distances the potential fluctuations are screened by the gate electrode. This comparison suggests that the spin droplets might originate due to the potential fluctuations at the $Si - SiO_2$ interface. However, without taking into account the intradroplet e-e interactions, it would be difficult to explain why the total spin is so large and why the SD size and spin remain unchanged over a wide density range.

In our view, the most likely reason for the emergence of SD states is the Stoner-type instability that occurs locally in the most depleted regions. The interaction parameter r_s is the largest in these regions, similar to the case of quantum dots discussed in Refs. [18–21,27]. An interesting issue is the "magic" total spin S of SDs that is independent of temperature and the average density. The experimentally estimated $S = 2$ [14] indicates that there are at least $n \geqslant 4$ electrons per SD. One might associate $n = 4$ with the four-fold valley and spin degeneracy of the electrons at the (100)Si surface. We think that the valley splitting at zero perpendicular field and valley degeneracy are irrelevant since for the samples studied $\Delta_v = 0.4$ K (for Si6-14) is less than the temperature of the measurements in Ref. [14]. The Zeeman splitting Δ_Z for spins 1/2 is also irrelevant since the measurements found in Ref. [14] as well as in this paper were performed at $\Delta_Z < k_B T$; under such conditions all spins and valleys are mixed. We therefore believe that the total spin and the number of electrons in a droplet are set by the intradroplet many-body interactions. Note that the maximum spin corresponds to a maximally antisymmetric coordinate wave function, which reduces Coulomb repulsion in restricted geometry.

Our observation that the SD states can recharge and quickly thermalize with the FL states indicates that the energy band of the SD states must be located in the vicinity of the Fermi level. This enables the T-independent elastic carrier exchange between the two bands via tunneling rather than

the temperature-induced activation. Since the collective states are energetically more favorable in the restricted area, the uppermost energy level of the SD state is likely to be located somewhat lower than E_F, by the binding energy Δ of the collective state.

In analogy with the conventional quantum dots and self-organized potential traps [44], here the confining potential of the SD state should be surrounded by a barrier preventing the dot from filling with electrons from the neighboring FL phase [Figs. 6(b) and 6(c)]. We believe that the SD states emerge near the maxima of the bare fluctuating potential, where a local collective (Stoner or spin-polarized Wigner) state emerges in the most depleted areas. This conclusion seems counterintuitive since conventional single-particle localized states are located *at the bottom of the potential landscape* and therefore fall into the band tail. The ground-state energy of SD becomes lower by the binding energy Δ than E_F of the surrounding Fermi sea [Fig. 6(c)]. The uppermost level of the collective state then goes down, below the peak of the potential hill (like a "volcano crater") leaving the surrounding potential barrier almost intact. Leaving aside the origin of the emerged "crater" (i.e., the SD energy level), the formation of the surrounding barrier is governed further by the conventional screening similar to that in Ref. [44].

The tunneling resistance R of the barrier and the SD size-dependent capacitance provide the characteristic RC time required for establishing equilibrium when T, H, or N are varied. Note that we ignore the strongly localized states positioned well below the Fermi energy, in the band tail, since they do not thermalize within the time of measurements. Accounting for these deep traps simply changes the overall density N by an offset that is temperature and field independent [40].

2. *Magnetic field variations of M and n*

The free energy of a multicomponent system is [1] $F = \sum_i \mu_i N_i$, where $\mu_{1,2} = \partial F/\partial N_{1,2}$ are the electrochemical potentials of the extended (FL) and localized (SD) components. In equilibrium $\mu_1(H,T)$ and $\mu_2(T,H)$ are equal, however, they may depend differently (and, in fact, do depend) on H and T.

Taking into account the result of the authors of Ref. [14] that the individual size of each SD (or quantum dot) does not change with field and temperature, the changes $N_2(B)$ may be induced only by variation of the number of SD states per unit area, i.e., by A_2. It is convenient to split the total free energy per unit area into three terms:

$$F = F_\mu + F_{\rm el} + F_H = [\mu_1 N_1 + \mu_2 N_2] \tag{2}$$

$$- \left[\frac{e^2 N_1^2}{2C_1} + \sum_j \frac{Q_{\rm SD}^2}{2C_{\rm SD}}\right] - \left[\frac{\chi_1 H^2}{2} + M_2 H\right]. \tag{3}$$

where $\mu_1 = \mu_2$ are the chemical potentials of each phase; $C_1 \approx (A_1)^{1/2}$ and $C_2 \approx (A_2)^{1/2}$ are the capacitances of the FL state and SD state per unit area; $M_2(H)$ is the magnetization of the SD state per unit area; $\chi^*(H)$ the spin susceptibility of the FL state per unit area; and the sum is over all SD states per unit area. The total electrostatic energy equals $N^2e^2/2\sqrt{A} = N^2e^2/2$ and is independent of H and T. In the free energy we took into account the electrostatic energy, magnetization energy of the mobile FL states and of the localized SD states [see Fig. 6(b)], and, for simplicity, neglected the mixing energy at the boundaries [10].

In equilibrium, we require [1]

$$\delta F = \delta F_\mu + \delta F_H + \delta F_{\rm el} = 0, \tag{4}$$

where variation of $F(H, N_i)$ is taken with respect to all relevant variables, $H_\parallel$, and N_i. In what follows we consider only the case of a fixed temperature since the available data [14,31] on the T dependencies of M, χ^*, and n_i have insufficient accuracy.

After regrouping terms in Eq. (4), dividing them by δH, and taking into account that $\delta N_1 = -\delta N_2$, Eq. (4) reduces to

$$\frac{\partial N_1}{\partial H}\left[\frac{N_1}{\tilde{D}_1} - \frac{N_2}{\tilde{D}_2} + \frac{\partial M_2}{\partial N_2}H\right] = -\frac{\partial \mu_2}{\partial H}N_2 - \frac{\partial \mu_2}{\partial H}H + M_2, \tag{5}$$

where $\tilde{D}_i = \partial N_i/\partial \mu_i$, and $D_i = \partial n_i/\partial \mu_i$ is the thermodynamic density of states for the ith component

$$\tilde{D}_i = \frac{\partial N_i}{\partial \mu_i} = A_i\frac{\partial n_i}{\partial \mu_i} + n_i\frac{\partial A_i}{\partial \mu_i} = A_i D_i + n_i\frac{\partial A_i}{\partial \mu_i}. \tag{6}$$

The third term in the square brackets of Eq. (5) may be neglected since it is by a factor of $\sim$70 smaller than the first one. We also neglected the terms (χH) and $(\partial\chi/\partial H)H^2$ in δF_H because of their smallness. Substituting $(\partial\mu/\partial H) = -(\partial M/\partial N)$ we obtain from Eq. (5)

$$\frac{\partial N_1}{\partial H}\left[\frac{N_1}{\tilde{D}_1} - \frac{N_2}{\tilde{D}_2}\right] = \frac{\partial M_2}{\partial N_2}N_2 + \frac{\partial M_2}{\partial H}H + M_2, \tag{7}$$

and after integrating both parts with respect to H:

$$N_1(H)\left[\frac{N_1}{\tilde{D}_1} - \frac{N_2}{\tilde{D}_2}\right] = \int dH\left[\frac{\partial M_2(H)}{\partial N}\frac{\partial N}{\partial N_2}N_2 + \frac{\partial M_2(H)}{\partial H}H + M_2(H)\right]. \tag{8}$$

Equation (8) relates changes in magnetization $M_2(H)$ of the SD localized states with the density variations $N_1(H)$ in the majority FL phase. In this equation $M_2(H)$, $\partial M_2/\partial H$, and $N_1(H)$ were determined experimentally (see Fig. 2), and $\partial M_2/\partial N$ may be found from Ref. [14] for a given density. The nominal carrier density $N_1 \propto n_{\rm SdH}$ is known from the SdH measurements, and D_1, in principle, may be calculated from the known renormalized effective mass m^* [32].

B. Comparison of the model with experimental data

The dependence $n_{\rm FL}(H) \propto N_1(H)$ calculated using Eq. (8) for the representative density 1.4×10^{11} cm^{-2} is shown in Fig. 7. It can be compared with direct experimental data of Fig. 2(c).

Although the $M_2(H_\parallel)$ and $n_{\rm SdH}(H_\parallel)$ data are available at slightly different densities, and the model has several simplifications, the calculated $\delta N_1(H)$ dependence captures the main features of the experimental data: the density of mobile electrons grows with field, reaches a maximum at approximately the same field of $1T$, and than slowly decreases. We conclude that there is a good qualitative agreement with the experimentally measured $n_{\rm FL}(H)$. On the right-hand side of Eq. (8) the second and third terms are positive and monotonically grow

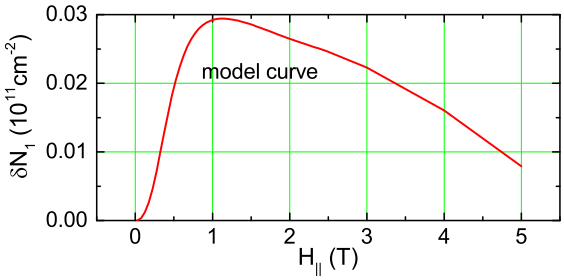

FIG. 7. Model curve $\delta N_1(H_\parallel)$ calculated from experimental data as described in the text.

with field. Only the first term is negative and, thus, results in the maximum and subsequent decrease in $N(H)$. This term is set to $(3.36 \pm 0.1) \times 10^{11}\ \mu_B/\mathrm{cm}^2$ to satisfy Eq. (8) and fit the observed decrease of $N(H)$.

For high densities, we believe that the complex shapes of the $\chi^*(H)$ and $n(H)$ dependencies [Figs. 3(e) and 4(d)] reflect the competition of several effects. One possibility is that the energy of the spin magnetization of the FL states $\chi^* H^2/2$ (which we assumed to be negligibly small at low and intermediate density and omitted for simplicity in our model) becomes comparable with (and may exceed) the magnetization energy of the SD states $M_2 H$. This is because the number of SD states vanishes as overall density increases [14,15]. Indeed, if we ignore the SD states magnetization for high densities, the monotonically growing with field FL magnetization energy $\chi^* H^2$ (in contrast to the sharply saturating $M_2 H$) in Eq. (6) would produce monotonic decrease of $n(H)$. The observed initial $n(H)$ decrease with field [Fig. 3(e) is consistent with such interpretation and indicates transfer of electrons from FL to the SD states. However, the accuracy and completeness of our data is insufficient to quantitatively treat these effects at high densities.

VII. DISCUSSION

(1) The similarity of the modeled and measured $n_{\mathrm{SdH}}(H)$ data justifies our approach. In the proposed scenario, the magnetization of the SD states causes changes in the free energy, which, in turn, cause redistribution of the carriers between the extended and localized states. The changes in the free energy also affect the magnetic energy of the delocalized states [detected experimentally as $\delta\chi^*(H)$]. These changes were neglected in our model since they are determined by a difference of two much larger terms in δF_H and the accuracy of our data is insufficient to calculate them. With rising density, the amount of the SD states diminishes [15], and the contribution of the delocalized FL states to magnetization energy becomes dominant. Apparently, this is the reason for the evolution of shape of the experimentally determined $n_{\mathrm{SdH}}(H)$ and $\chi^*(H)$ dependencies at the highest carrier density $10 \times 10^{11}\ \mathrm{cm}^{-2}$ (see Fig. 5).

(2) It is worth noting that for a 2D FL system, due to the electron-electron interaction corrections in the diffusive regime $T\tau \ll 1$, the spin susceptibility is expected to vary smoothly and insignificantly $\propto -\ln(g\mu_B H/2\pi k_B T)$ in fields $g\mu_B H_\parallel \ll k_B T$ [31,45] [see also Eqs. (A1) and (A2) in Appendix A]. With the approach to the field of complete spin polarization of the 2D FL system [$H_p \sim 2E_F/g\mu_B \sim$ 10–20 T for the relevant densities $(1\text{–}2) \times 10^{11}\ \mathrm{cm}^{-2}$], the spin susceptibility is predicted to strongly increase [30]. Anyhow, χ^* in a single-phase 2D FL system is not expected to exhibit strong variations in weak fields of the order of $k_B T/\mu_B$.

(3) Variation of the carrier concentration in 2D gated systems [46,47] in a perpendicular field is a well-known effect. The variations $\delta N(H)$ at a constant gate voltage are commonly treated within the framework of the single-phase picture and related to the chemical potential jumps $\delta\mu(H)$ between the Landau levels in the spectrum of the FL state. Alternatively, in thermodynamic magnetization measurements in the weak in-plane field [14,48], recharging of the gated 2D structure was predominantly caused by the SD states, whereas the transport response of the mobile FL states was not measured. Therefore, it is possible to treat the results within single-phase model and almost ignore the FL states.

In the current paper we measured and analyzed both the transport and thermodynamic data and found that the conventional single-phase approach is not capable to explain the two sets of data even qualitatively. This is because in the parallel field the magnetization of the SD subsystem exceeds (or at least, is comparable with) the Pauli magnetization of mobile electrons.

(4) The carrier redistribution between the localized and extended states is common for many types of field-effect semiconductor-insulator structures [49,50]. This effect typically "freezes out" at lowering temperatures because it requires temperature activation from the tail states to the Fermi level. Here we reported the effect of redistribution that persists down to ultralow temperatures. We associate this temperature-independent effect with elastic tunneling between the states of different nature but with the same energy.

(5) The carrier redistribution between two phases in the 2D system is not easy to determine by other techniques. For example, the capacitance measurements taken at frequencies 0–10^6 Hz (1 nF, 1 kOhm/□) probe the total charge density that includes both SD and mobile states. To separate the SD and FL states, the capacitance measurements should be done at frequency of 10^{10}–10^{12} Hz, inaccessible for the gated structure. We already noted that the FL density deduced from SdH oscillations in the phase-separated system is determined by the local density in the FL lakes (where the carriers possess the highest relaxation time) rather than by the total density; this picture holds until the delocalized states (FL lakes) percolate. For the gated 2D system, the difference of the local density within the FL lakes and within the SD areas is negligibly small because of the associated electrostatic energy and neutrality requirement.

The difference between the overall charge in the 2D system (determined from recharging measurements) and the mobile FL carrier density (local charge density) deduced from SdH/QHE was measured in Ref. [46] and found to be less than 2%, i.e., within the experimental uncertainty. Note that the Hall voltage measurements also cannot shed light on the mobile and SD carrier density since the Hall voltage becomes irrelevant to the carrier density at the verge of the localization transition (the so-called "Hall insulator") [51].

(6) Though the $\chi^*(H_\parallel)$ changes for mobile carriers were not calculated in our model because of the smallness of the corresponding magnetic energy changes, the changes should occur due to the following thermodynamic arguments. The microscopic mechanism behind these changes is as follows: the carriers in the SD states have their spins aligned ferromagnetically along the field, and when they tunnel elastically into the Fermi sea, they should join the spin-minority subband. As a result, the spin polarization degree $(n\uparrow - n\downarrow)/n$ measured from the SdH oscillations beating diminishes; the spin susceptibility reported here has been found from this parameter. Further slow restoring of χ^* with $H_\parallel$-field presumably reflects the spatially averaged density of states for the SD's. Qualitatively, we conjecture that the average width of the uppermost energy level in the SD states amounts to ~4 K, as estimated from the corresponding restoration field of 3 T in Fig. 2.

(7) The observed $\chi^*(H_\parallel)$ variations (Figs. 1 and 2) indicate that a widely used approach for determining the spin susceptibility from the monotonic magnetoresistance measurements in parallel magnetic fields [28,29] might result in significant errors. Indeed, the $\langle g^* m^*(H_\parallel)\rangle$ averaged over a wide field range (from 0 to the spin polarization field H_p) is about 10% smaller than the zero-field value $g^* m^*(H \to 0)$. If the monotonic magnetoresistance is measured in weaker fields $H \leqslant H_p$, the underestimation of χ^* caused by finite $H_\parallel$ may be even greater (e.g., it may reach 15% for the degree of spin polarization ≈0.05–0.1).

VIII. CONCLUSION

We observed and explored an unexpected sharp field dependencies of the FL spin susceptibility $\chi^*(H_\parallel)$ and the density $n_{\mathrm{SdH}}(H)$ of the mobile electrons in the regime of strong interelectron interactions ($r_s = 7.3$–3.4). The two effects correlate well with each other and with the thermodynamic magnetization of the localized SD states. We suggested a simple phenomenological two-phase model that links the changes in the density of the mobile electrons to the magnetization of the collective localized states spatially separated from the extended FL states. The qualitative agreement of the model with experimental data suggests that the variations of $n_{\mathrm{SdH}}(H)$ and $\chi^*(H)$ with the in-plane field are caused by magnetization of the minority phase of collective localized states. Thus, our results provide the solid evidence for the phase separation in the interacting 2D electron system even at relatively high carrier densities, deeply in the "metallic" regime of high conductivity [$\sigma = (3$–$80) \times (e^2/h)$] [52].

Our results also explain a long-standing disagreement between the experimentally measured values of the spin-susceptibility and g^*-factor obtained in weak and strong magnetic fields. Though the presented empiric phenomenological model qualitatively explains the data at intermediate densities, for the quantitative analysis a microscopic theoretical consideration is required that would take into account the energy spectrum of the SD states.

ACKNOWLEDGMENTS

V.P. acknowledges fruitful discussion with A. L. Rakhmanov. This work was supported by the RFBR, Project No. 18-02-01013, and fulfilled within the state assignment of the Ministry of Science and Higher Education of the Russian Federation (Project "Physics of high temperature superconductors and novel quantum materials" No 0023-2019-0005).

APPENDIX A: THEORETICALLY PREDICTED $\chi(H)$ DEPENDENCE FOR THE 2D FERMI LIQUID

The Fermi liquid quantum correction to $\chi(H)$ in the diffusive interaction regime at weak fields and not too low temperatures, $(1+\gamma_2)g\mu_B H_\parallel/(2\pi k_B T) \ll 1$, to the second order in h is given in Ref. [31]:

$$\frac{\delta\chi^*(H_\parallel)}{\chi^*(0)} = -\frac{1}{\sigma_{xx}}\frac{\zeta(3)}{\pi^2} g_v^2[(1+\gamma_2)^3 - 1]h^2, \tag{A1}$$

where $h = g\mu_B H/2\pi k_B T$, g_v - valley degeneracy, $\gamma_2 = -F_0^\sigma/(1+F_0^\sigma)$, F_0^σ is the FL coupling constant in the particle-hole triplet channel, and $\chi^*(0) = g_v\mu_B^2 m^*/[\pi(1+F_0^\sigma)]$ is the spin susceptibility of the FL at $H = 0$ and $T = 0$. For stronger fields or lower temperatures $2\pi k_B T \ll (1+\gamma_2)g\mu_B H_\parallel$,

$$\frac{\delta\chi(H_\parallel)}{\chi(0)} \approx -\frac{1}{\sigma_{xx}}\frac{g_v^2\gamma_2}{\pi^2}\ln(g\mu_B H_\parallel \tau), \tag{A2}$$

which is consistent with the theory by Al'tshuler and Zyuzin [45].

Equations (1) and (2) predict $\chi(H)$ to *monotonically decrease* with $H_\parallel$, unlike the experimentally observed V-shaped $\chi^*(H)$ dependence (see Fig. 1). Within an alternative approach, by taking into account the spin polarization dependence of the exchange and kinetic energy, Zhang and Das Sarma found that χ^* should *monotonically grow* with $H_\parallel$ almost up to the field of complete spin polarization [30].

We stress that (i) the characteristic field (typically, $H_\parallel \sim 1$ T, see Fig. 1) of the observed $\chi^*(H)$ minimum is much weaker than the field of complete spin polarization of a pure 2D system $H_p = 2E_F/g\mu_B \approx 10.88(N/10^{11})$[T], and (ii) there is no other characteristic field besides H_p in a homogeneous single-phase system. We conclude that the predicted magnetic field dependencies due to interaction corrections and spin-polarization are irrelevant (to the first approximation) to the observed sharp changes of $\chi^*(H)$.

APPENDIX B: THERMODYNAMICS OF THE SINGLE-PHASE STATE

Consider the simplest single-phase picture that is traditionally applied to the capacitive type measurements with gated 2D systems. Namely, we consider the total charge density [47,48]

$$N = \frac{C_0}{e}\left(V_g - \frac{\mu_{2\mathrm{D}} - \mu_g}{e}\right), \tag{B1}$$

where $\mu_{2\mathrm{D}}$ and μ_g are the electrochemical potentials of the electrons in the 2D layer and the gate (Al film), V_g is the gate voltage, and C_0 is the capacitance between the 2D layer and the gate. Here we neglect slight renormalization of the geometric capacitance by the electron compressibility [48].

Taking variations with in-plane magnetic field, we obtain

$$\frac{e^2}{C_0}\frac{\partial N}{\partial H} = +\frac{\partial M}{\partial N}. \tag{B2}$$

Here, we used the Maxwell relation $\partial\mu_{2D}/\partial H = -\partial M/\partial N$ and disregarded the "diamagnetic shift," i.e., magnetic field dependence of C_0. This diamagnetic shift contributes to $\partial M/\partial N$ less than $0.05\mu_B$ at low densities and further drops as N increases [48]. This equation predicts direct proportionality between the magnetic field variation of dN/dH and the magnetization per electron $\partial M(H)/\partial N$. Both quantities were experimentally measured: $dN(H)/dH$ is shown in Fig. 8 and $\partial M(H)/\partial N$ in Fig. 6(a). Clearly, there is little in common between the two dependencies, and we conclude that the single-phase picture is inadequate for explaining the experimental results.

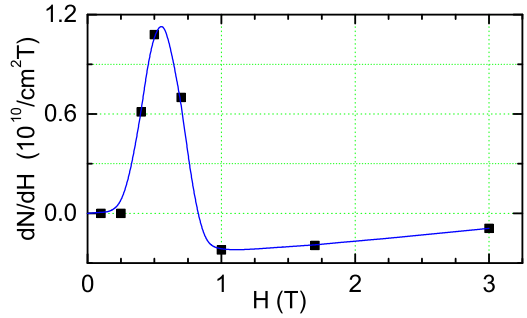

FIG. 8. Example of the magnetic field dependence of $dN(H)/dH$ calculated from Fig. 4(c). Sample Si6-14. $N(0) = 1.61 \times 10^{11}$ cm^{-2}.

[1] E. M. Lifshits and L. P. Pitaevskii, *Statistical Physics, Part II*: *Theory of the Condensed State*, L. D. Landau Course of Theoretical Physics (Pergamon, Oxford, New York, 1986), Vol. IX.

[2] D. Pines and P. Nozieres, *The Theory of Quantum Liquids* (W.A. Banjamin, New York-Amsterdam, 1966).

[3] C. M. Varma, Z. Nussinov, and W. van Saarloos, Phys. Rep. **361**, 267 (2002).

[4] The dimensionless ratio of the Coulomb interaction energy to the Fermi energy $r_s = E_{ee}/g_v E_F = 2.63 \times (10^{12}\,\mathrm{cm}^{-2}/n)^{1/2}$. This value takes into account the valley degeneracy $g_v = 2$ in (100)Si.

[5] B. Spivak, Phys. Rev. B **67**, 125205 (2003); B. Spivak and S. A. Kivelson, *ibid.* **70**, 155114 (2004).

[6] V. Dobrosavljevic, E. Abrahams, E. Miranda, and S. Chakravarty, Phys. Rev. Lett. **79**, 455 (1997).

[7] S. Chakravarty, L. Yin, and E. Abrahams, Phys. Rev. B **58**, R559 (1998).

[8] S. Chakravarty, S. Kivelson, C. Nayak, and K. Voelker, Phil. Mag. B **79**, 859 (1999).

[9] V. A. Khodel, J. W. Clark, and M. V. Zverev, Phys. Rev. B **102**, 201108(R) (2020).

[10] J. Lorenzana, C. Castellani, and C. Di Castro, Phys. Rev. B **64**, 235127 (2001); **64**, 235128 (2001).

[11] A. V. Kornilov, V. M. Pudalov, Y. Kitaoka, K. Ishida, G.-Q. Zheng, T. Mito, and J. S. Qualls, Phys. Rev. B **69**, 224404 (2004).

[12] Ya. A. Gerasimenko, S. V. Sanduleanu, V. A. Prudkoglyad, A. V. Kornilov, J. Yamada, J. S. Qualls, and V. M. Pudalov, Phys. Rev. B **89**, 054518 (2014).

[13] S. Ilani, A. Yacobi, D. Mahalu, and H. Shtrikman, Science **292**, 1354 (2001).

[14] N. Teneh, A. Yu. Kuntsevich, V. M. Pudalov, and M. Reznikov, Phys. Rev. Lett. **109**, 226403 (2012).

[15] L. A. Morgun, A. Yu. Kuntsevich, and V. M. Pudalov, Phys. Rev. B **93**, 235145 (2016).

[16] V. M. Pudalov, L. A. Morgun, and A. Yu. Kuntsevich, J. Supercond. Novel Magn. **30**, 783 (2017).

[17] Y. V. Stadnik and O. P. Sushkov, Phys. Rev. B **88**, 125402 (2013).

[18] E. Eisenberg and R. Berkovits, Phys. Rev. B **60**, 15261 (1999).

[19] P. W. Brouwer, Y. Oreg, and B. I. Halperin, Phys. Rev. B **60**, R13977 (1999).

[20] I. L. Kurland, I. L. Aleiner, and B. L. Altshuler, Phys. Rev. B **62**, 14886 (2000).

[21] B. N. Narozhny, I. L. Aleiner, and A. I. Larkin, Phys Rev. B **62**, 14898 (2000).

[22] J. I. Väyrynen, M. Goldstein, and L. I. Glazman, Phys. Rev. Lett. **110**, 216402 (2013).

[23] J. I. Väyrynen, M. Goldstein, Y. Gefen, and L. I. Glazman, Phys. Rev. B **90**, 115309 (2014).

[24] I. S. Burmistrov, Y. Gefen, D. S. Shapiro, and A. Shnirman, Phys. Rev. Lett. **124**, 196801 (2020).

[25] D. H. Cobden, C. H. W. Barnes, and C. J. B. Ford, Phys. Rev. Lett. **82**, 4695 (1999).

[26] A. Ghosh, C. J. B. Ford, M. Pepper, H. E. Beere, and D. A. Ritchie, Phys. Rev. Lett. **92**, 116601 (2004).

[27] M. C. Rogge, E. Räsänen, and R. J. Haug, Phys. Rev. Lett. **105**, 046802 (2010).

[28] S. A. Vitkalov, H. Zheng, K. M. Mertes, M. P. Sarachik, and T. M. Klapwijk, Phys. Rev. Lett. **87**, 086401 (2001).

[29] A. A. Shashkin, S. V. Kravchenko, V. T. Dolgopolov, and T. M. Klapwijk, Phys. Rev. Lett. **87**, 086801 (2001).

[30] Y. Zhang and S. Das Sarma, Phys. Rev. Lett. **96**, 196602 (2006).

[31] V. M. Pudalov, A. Yu. Kuntsevich, M. E. Gershenson, I. S. Burmistrov, and M. Reznikov, Phys. Rev. B **98**, 155109 (2018).

[32] V. M. Pudalov, M. E. Gershenson, H. Kojima, N. Butch, E. M. Dizhur, G. Brunthaler, A. Prinz, and G. Bauer, Phys. Rev. Lett. **88**, 196404 (2002).

[33] V. M. Pudalov, M. E. Gershenson, and H. Kojima, Phys. Rev. B **90**, 075147 (2014).

[34] I. M. Lifshitz and A. M. Kosevich, Zh. Eks. Teor. Fiz. **29**, 730 (1955); A. Isihara, L. Smrčka, J. Phys. C: Solid State Phys. **19**, 6777 (1986).

[35] N. N. Klimov, D. A. Knyazev, O. E. Omel'yanovskii, V. M. Pudalov, H. Kojima, and M. E. Gershenson, Phys. Rev. B **78**, 195308 (2008).

[36] V. M. Pudalov, G. Brunthaler, A. Prinz, and G. Bauer, JETP Lett. **65**, 932 (1997).

[37] D. Simonian, S. V. Kravchenko, M. P. Sarachik, and V. M. Pudalov, Phys. Rev. Lett. **79**, 2304 (1997).
[38] V. M. Pudalov, G. Brunthaler, A. Prinz, and G. Bauer, Physica B **249-251**, 697 (1998).
[39] S. V. Kravchenko, D. Simonian, M. P. Sarachik, A. D. Kent, and V. M. Pudalov, Phys. Rev. B **58**, 3553 (1998).
[40] T. Ando, A. B. Fowler, and F. Stern, Rev. Mod. Phys. **54**, 437 (1982).
[41] S. A. Vitkalov, M. P. Sarachik, and T. M. Klapwijk, Phys. Rev. B **65**, 201106(R) (2002).
[42] A. Gold and V. T. Dolgopolov, J. Phys.: Condens. Matter **14**, 7091 (2002).
[43] A. Yu. Kuntsevich, Y. V. Tupikov, V. M. Pudalov, and I. S. Burmistrov, Nat. Commun. **6**, 7298 (2015).
[44] V. Tripathi and M. P. Kennett, Phys. Rev. B **74**, 195334 (2006).
[45] B. L. Altshuler, A. G. Aronov, and A. Yu. Zyuzin, Pis'ma ZhETF **35**, 15 (1982) [JETP Lett. **35**, 16 (1982)].
[46] V. M. Pudalov, S. G. Semenchinskii, and V. S. Edelman, Pis'ma ZhETF **39**, 474 (1984) [JETP Lett. **39**, 576 (1984)].
[47] V. M. Pudalov, S. G. Semenchinskii, Pis'ma ZhETF **44**, 526 (1986) [JETP Lett. **44**, 677 (1986)].
[48] M. Reznikov, A. Yu. Kuntsevich, N. Teneh, and V. M. Pudalov, JETP Lett. **92**, 470 (2010).
[49] H. Sirringhaus, Adv. Mater. **21**, 3859 (2009).
[50] B. Lee, A. Wan, D. Mastrogiovanni, J. E. Anthony, E. Garfunkel, and V. Podzorov, Phys. Rev. B **82**, 085302 (2010).
[51] V. M. Pudalov, M. D'Iorio, and J. Campbell, Pis'ma ZhETF **57**, 592 (1993) [JETP Lett. **57**, 608 (1993)].
[52] V. M. Pudalov, G. Brunthaler, A. Prinz, and G. Bauer, Phys. Rev. B **60**, R2154 (1999).